Supporting information for

Enhancing vibrational light-matter coupling strength beyond the molecular concentration limit using plasmonic arrays

Manuel Hertzog,[†] Battulga Munkhbat,[‡] Denis Baranov,[‡] Timur Shegai,[*,‡] and Karl Börjesson[*,†]

†*Department of Chemistry and Molecular Biology, University of Gothenburg, Kemigården 4, 412 96, Gothenburg, Sweden*

‡*Department of Physics, Chalmers University of Technology, 412 96, Gothenburg, Sweden*

E-mail: timurs@chalmers.se; karl.borjesson@gu.se

Contents

S1 Methods

S1.1 Cavity preparation

Fabry-Pérot cavities were produced using a demountable liquid cell for IR spectroscopy (Omni Cell, Specac) with CaF_2 and ZnSe optical windows. The substrates were cleaned with acetone and isopropanol (IPA), and dried under nitrogen. The gold mirrors (10 nm) were deposited using a DC magnetron sputterer (HEX, Korvus Technologies) or electron beam (e-beam) evaporator. Then, a 450 nm SiO_2 layer was deposited by sputtering on top of the freshly prepared bottom gold mirror. Lattice arrays of gold nanorods with various lengths and densities were fabricated using a standard e-beam lithography (EBL) technique. In brief, a 110 nm of poly(methyl methacrylate) PMMA layer was spin coated on top of the SiO_2 layer, and baked at 180 °C for 5 min. Then, samples were exposed using a JEOL JBX 9300FS electron beam lithography system according to pre-designed pattern of nanorods with a fixed width of 150 nm and various lengths, ranging from 1100 nm to 1500 nm with a step of 100 nm. The edge to edge distances were 1000 nm and 150 nm along the longer and shorter axis of the rods, respectively. After the e-beam exposure, the samples were developed under a MIBK:IPA (1:3) solution and rinsed with IPA, and dried under nitrogen gas. Afterwards, 2 nm of chromium and 40 nm of gold were deposited with e-beam evaporation. Lastly, a lift-off process was done in acetone at 60 °C for ca. 30 min, and rinsed with IPA and water, to form the gold nanorods. The physical distance between the mirrors was controlled using a Mylar spacer (Specac) of 6 µm and the fine adjustment of the thickness was done using adjustment screws on the microfluidic cell. Finally, hexanal (Sigma-Aldrich) and 4-butylbenzonitrile (Sigma-Aldrich) were injected into the cavity using a syringe connected to the inlet of the cell. All chemicals were used without further purification.

S1.2 Optical characterization

Infrared spectra were recorded using an FT-IR microscope (Hyperion 3000, Bruker), using a Schwarzschild-objective 15x objective (NA=0.4) and a linear polarizer (Specac GS57016) parallel

and perpendicular to the long axis of the nanorods, connected to an FT-IR spectrometer (Vertex 70v, Bruker) in reflection or transmission mode. All measurements were recorded with a liquid nitrogen cooled MCT detector at a resolution of $4\,\mathrm{cm}^{-1}$ using 512 scans. Furthermore, ATR spectra were recorded using an FT-IR spectrometer (Invenio-R, Bruker) coupled to a PLATINUM ATR accessory (Bruker). The ATR spectra were recorded using a DLaTGS detector with a resolution of $4\,\mathrm{cm}^{-1}$ and 64 scans. Morphology of the samples was characterized using a Zeiss (Germany) scanning electron microscope (SEM ULTRA 55 FEG).

S1.3 Numerical modelling

FDTD simulations of the electromagnetic response of the coupled plasmon–cavity and plasmon-molecule-cavity systems were performed using a commercial software (FDTD Solutions, Lumerical, Inc., Canada). Transmission and absorption spectra, as well as electromagnetic field distributions, were obtained with the use of a linearly polarized normally incident plane wave source and periodic boundary conditions. The plane wave was polarized either along the nanorods or perpendicular to them. The permittivity of gold was approximated by interpolating the experimental data from Johnson and Christie[1] in the range 3 µm to 8 µm. The mesh parameter was set to 4 in all simulations.

In order to obtain the optical response of hexanal and 4-butylbenzonitrile in the infrared region a multi-Lorentz oscillator model was used:[2]

$$\tilde{n}(k) = \sqrt{n_b^2 - \sum_{j=0}^{N} \frac{f_j}{k^2 - k_{0j}^2 + ik\gamma_j}} \tag{S1}$$

where, n_b is the background refractive index, f_j is the oscillator strength, k_{0j} is the resonant wave vector and γ_j is the damping constant, i.e. the full width at half maximum of the j^{th} oscillator.

S1.4 Cavity thickness determination

The cavity thickness d was measured using the following equation:

$$d = \frac{q}{2n}\left(\frac{\lambda_i\lambda_j}{\lambda_i - \lambda_j}\right) \tag{S2}$$

where, $\lambda_{i,j}$ are the wavelengths of the Fabry-Pérot mode, n the refractive index and q is an integer number given by $q = j - i$.

Table 1. Measured thicknesses of the FP cavities.

Cavity	FP/rods	FP/hex	FP/4-butyl	FP/rods/hex	FP/rods/4-butyl
d [μm]	10.8	14.9	16.3	8.45	10.4

S1.5 Hamiltonian analysis

The eigenstates of the coupled cavity-molecular system are modelled with the multimode coupled-harmonic oscillator Hamiltonian, including M lowest Fabry-Pérot modes, and the single harmonic oscillator describing the collective molecular resonance. The cavity is described by a set of M orthogonal Fabry-Pérot eigenmodes with equidistant frequencies $\omega_m = m\omega_1$, each coupling to the molecular resonance with a certain coupling constant. For pure molecular samples, all the N molecules residing within the cavity can be roughly approximated by a single collective harmonic oscillator with the resonant frequency of a single molecule ω_0, and the collective dipole moment $\mu\sqrt{N}$ (this approximation is rather crude, but for the purposes of extracting collective molecular, plasmonic, and intermixed situations, is sufficiently adequate). The Hamiltonian takes the form:

$$\hat{H}_{mol} = \sum_{m=1}^{M} \hbar\omega_m \hat{a}_m^\dagger \hat{a}_m + \hbar\omega_0 \hat{b}^\dagger \hat{b} + \sum_{m=1}^{M} \hbar g_m (\hat{a}_m^\dagger \hat{b} + \hat{a}_m \hat{b}^\dagger) \tag{S3}$$

where $\hat{a}$ and $\hat{b}$ are the annihilation operators of the m-th cavity mode and that of the molecular resonance, respectively, and g_m is the coupling constant to m-th cavity mode.

The coupling constant to the m-th cavity mode is given by the standard expression follow-

ing from the expansion of the minimal coupling Hamiltonian in the Coulomb gauge:[3,4] $g_m = \mu\sqrt{\rho}\mathcal{E}_{vac}\omega_0/\omega_m$, where μ is the dipole moment of transitions with density ρ, and $\mathcal{E}_{vac}$ is the cavity vacuum field. Each molecule in the cavity, in principle, will experience a different vacuum field depending on its position. But to simplify the analysis, we will assume that all molecules experience the same average vacuum field $\mathcal{E}_{vac} \sim \sqrt{\hbar\omega_m/L_{cav}}$. Thus, the coupling strength with the m-th cavity mode takes the form $g_m = g_0\sqrt{\hbar\omega_m}\omega_0/\omega_m$, where g_0 is a scaling constant that involves the molecular dipole moment, the molecular concentration, and the cavity mode volume.

The coupled Fabry-Pérot system exhibits transmission peaks at its polaritonic resonances, corresponding to the eigenvalues of its effective Hamiltonian. We estimate the cavity-molecule coupling strength by fitting the energies of the transmission peaks by the eigenvalues of Hamiltonian Eq. S3 accounting for $M = 20$ lowest cavity modes. Simply estimating the number of supported FP modes as $M \sim \omega_{plasma}/\omega_1$ with ω_{plasma} being the plasma frequency of the mirror's metal, we find that these cavities support over hundred eigenmodes; however, the energy spectrum of Eq. S3 quickly converges and the presence of high energy modes only weakly affects the eigenvalues in the relevant spectral range. The cavity thickness L_{cav} for each sample was first roughly estimated by counting the number of transmission peaks q away from the molecular resonance in a certain wavelength range $\lambda_1 \ldots \lambda_2$; next, it was varied during the fitting to yield better agreement between measured and theoretical dispersions.

Spectra of the cavity-plasmon samples w/o molecules are analyzed in a similar fashion by replacing the single collective molecular resonance with a single mode plasmonic mode. The nanorod array can be described by a single harmonic oscillator with energy ω_{pl} which disperses with the nanorod length L_{rod} (Figure S3a). Since it is positioned in a specific horizontal plane inside the cavity at a height z above the bottom mirror, the coupling strength takes the form $g_m = g_0\sqrt{\hbar\omega_m}\sin\frac{zm\pi}{L_{cav}}\omega_0/\omega_m$, which takes into account the transverse distribution of the vacuum cavity field. Strictly speaking, the coupling strength will also disperse with the nanorods length. Longer nanorods will have a larger transition dipole moment, but the increasing length at the same time reduces their surface density. The exact scaling law of the nanorod dipole moment with length

is not known, but we will assume for simplicity that the product $\mu\sqrt{\rho}$ is constant in the studied range of L_{rod} between 1100 and 1500 nm (for comparison, we observed less than 50% variation of this product upon an octave variation of nanorods length in a similar system[4]). Hence, we replace ω_0 in the Hamiltonian (Eq. 1) with ω_{pl} and substitute the corresponding coupling strength; note that $n_b = 1$ (the background refractive index of the cavity medium) for plasmonic samples.

Full three-components systems (cavity + nanorod arrays + molecules) are modelled with the same JC Hamiltonian, where the plasmon-molecule hybrid is described as a single collective oscillator characterized by the plasmon energy ω_0 that couples to Fabry-Pérot cavity modes with coupling strength g_m. The coupling strength of this hybrid oscillator to the m-th cavity mode takes the form $g_m = g_0\sqrt{\hbar\omega_m}\sin\frac{zm\pi}{L_{cav}}\omega_0/\omega_m$, where z is the position of the nanorod array above the bottom mirror (exactly like in the cavity-nanorod system). This approach is justified by the fact that the plasmon provide most of the coupling strength.

S2 Additional figures

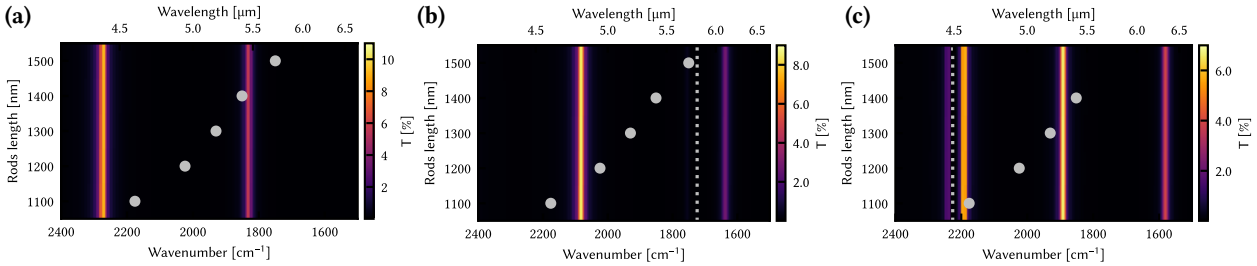

Figure S1. (a)-(c) Simulated transmission spectra of the gold rods inside the Fabry-Pérot cavity, without molecules, with hexanal, and with 4-butylbenzonitrile, respectively. All three are simulated with a polarizer perpendicular to the long axis of the rods. The gray dashed line indicates the absorption band of interest of the molecules and the gray dots indicates the absorption maximum of the bare plasmons.

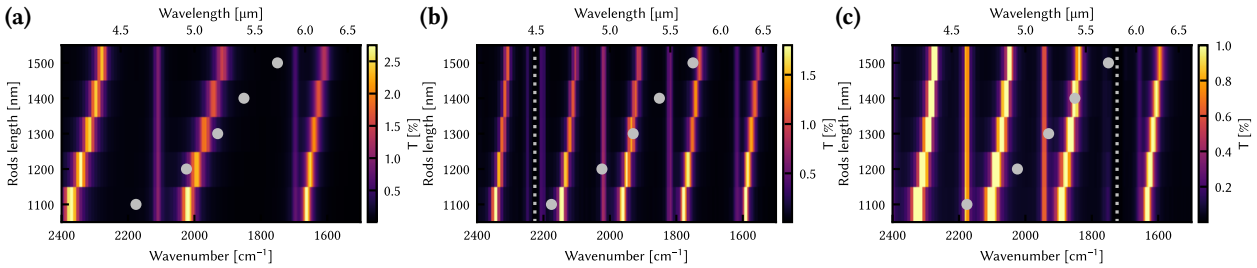

Figure S2. (a)-(c) Simulated transmission spectra of the gold rods inside the Fabry-Pérot cavity, without molecules, with hexanal, and with 4-butylbenzonitrile, respectively. All three are simulated with a polarizer at 20° relatively to the long axis of the rods. The gray dashed line indicates the absorption band of interest of the molecules and the gray dots indicates the absorption maximum of the bare plasmons.

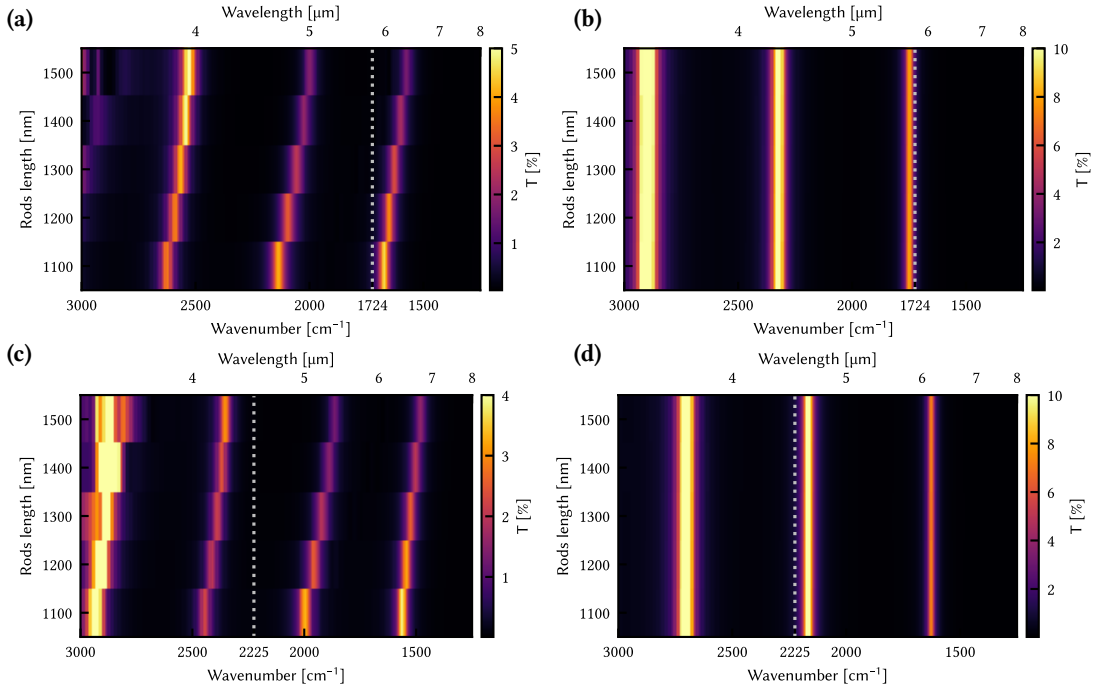

Figure S3. Simulated transmission spectra with the oscillator strength set to zero of: **(a-b)** the coupled rods in the FP cavity with hexanal, with the polarisation along the rods axis and perpendicular, respectively; **(c-d)** the coupled rods in the FP cavity with 4-butylbenzonitrile, with the polarisation along the rods axis and perpendicular, respectively.

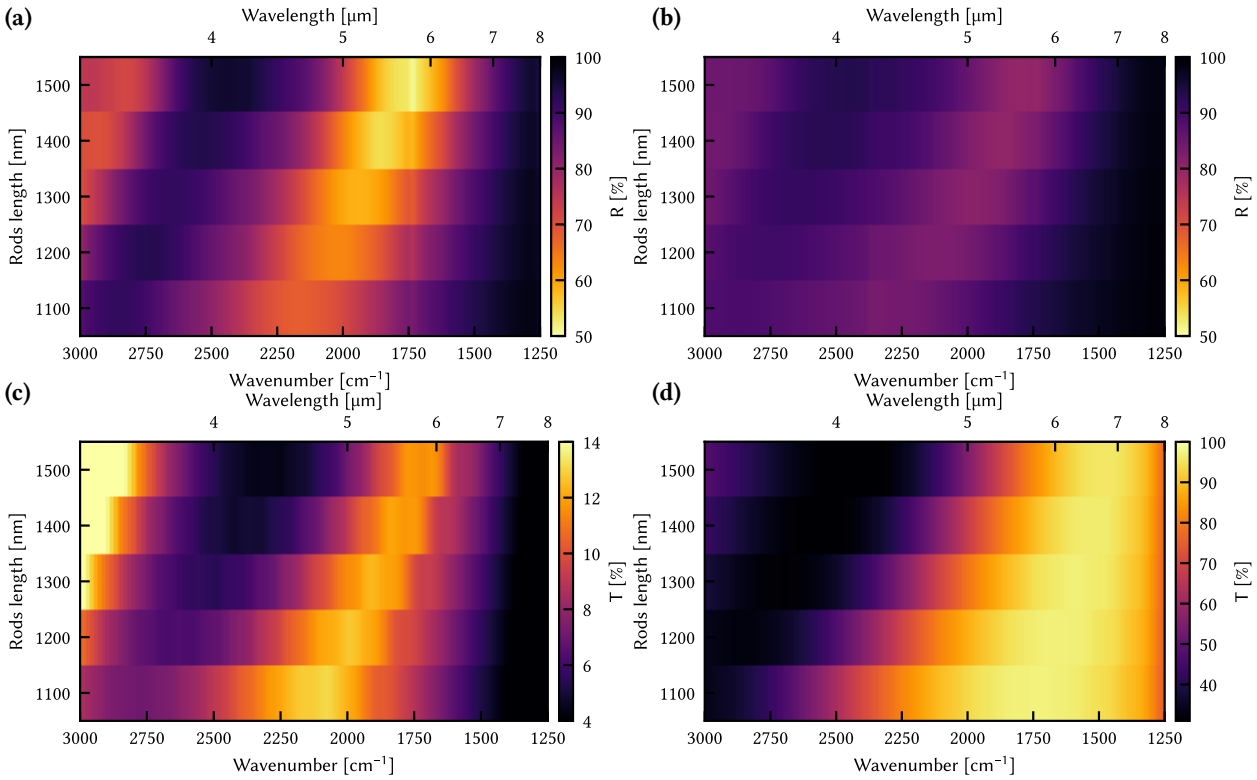

Figure S4. **(a)-(b)** Reflection map of the gold arrays with the polarizer along and perpendicular to the rods long axis, respectively. **(c)-(d)** Simulated transmission spectra of the gold arrays with and without a bottom mirror, respectively.

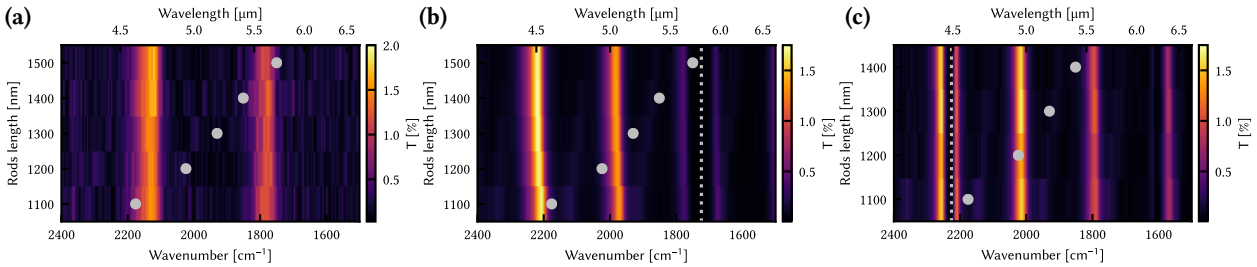

Figure S5. **(a)-(c)** Transmission maps of the gold nanorods inside the Fabry-Pérot cavity, containing air, hexanal, or 4-butylbenzonitrile, respectively. All three were measured with a polarizer perpendicular to the long axis of the rods. The gray dashed line indicates the absorption band of interest of the molecules and the gray dots indicate the plasmon absorption maximum.

Table 2. FWHM of relevant transitions and FP modes. All linewidths are given in cm^{-1} and rod lengths in nm.

media in cavity	air		hexanal		4-butylb
FP mode FWHM*	84 ± 7.3		42 ± 1.6		31.3 ± 2.9
Rod length [nm]	1100	1200	1300	1400	1500
Bare plasmon [cm^{-1}]	1120	1032	882	745	621
FP/rods polariton [cm^{-1}]	69.5 ± 0.5	72 ± 6	72.5 ± 0.5	66†	66†
FP/rods/hexanal polariton [cm^{-1}]	41.3 ± 7.4	41.3 ± 4.5	40.5 ± 2.5	36.3 ± 4.5	39.5 ± 1.5
FP/rods/4-butylb polariton [cm^{-1}]	34.3 ± 2.9	34 ± 2.8	33.5 ± 1.5	29 ± 4	/

* Measured next to the array
† Too low signal-to-noise to measure more than 1 peak

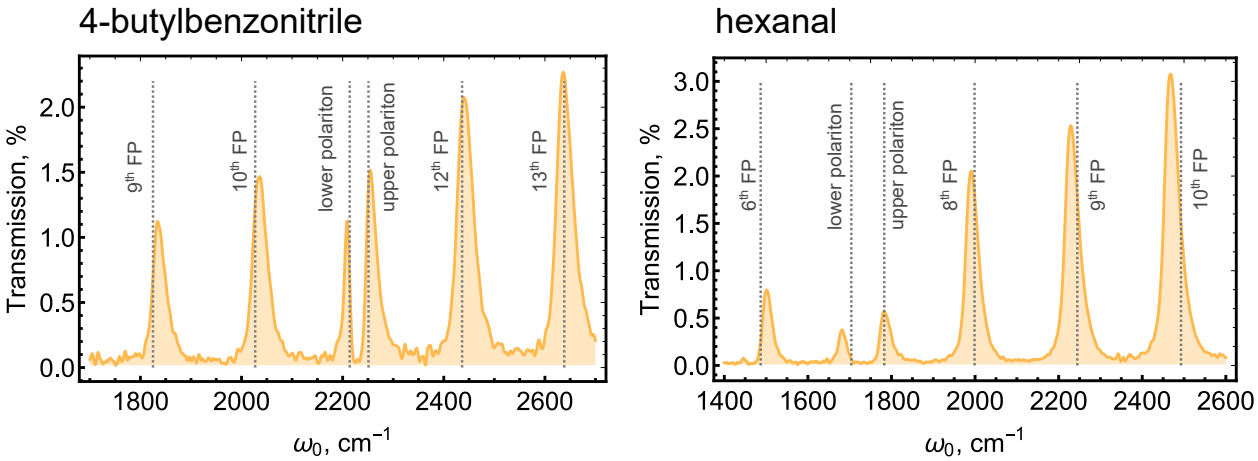

Figure S6. Transmission spectra of filled cavities without the gold nanorods arrays. The vertical dotted lines represent fitting of the transmission peaks of the cavity+molecules systems with the Hamiltonian eigenvalues.

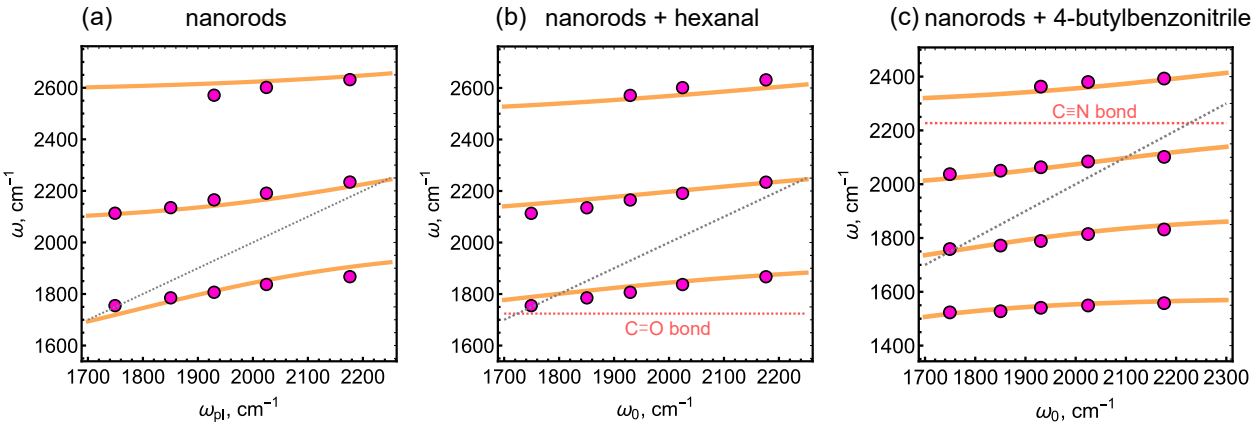

Figure S7. Fits of the measured dispersion of transmission peaks of the coupled systems (circles) with eigenvalues of the multimode Jaynes-Cummings Hamiltonian (curves) revealing a set of anti-crossings between polaritonic states.

References

(1) Johnson, P. B.; Christy, R. W. Optical Constants of the Noble Metals. *Phys. Rev. B* **1972**, *6*, 4370–4379.

(2) George, J.; Chervy, T.; Shalabney, A.; Devaux, E.; Hiura, H.; Genet, C.; Ebbesen, T. W. Multiple Rabi Splittings under Ultrastrong Vibrational Coupling. *Phys. Rev. Lett.* **2016**, *117*, 153601.

(3) Liberato, S. D. Light-Matter Decoupling in the Deep Strong Coupling Regime: The Breakdown of the Purcell Effect. *Phys. Rev. Lett.* **2014**, *112*, 016401.

(4) Baranov, D. G.; Munkhbat, B.; Zhukova, E.; Bisht, A.; Canales, A.; Rousseaux, B.; Johansson, G.; Antosiewicz, T. J.; Shegai, T. Ultrastrong coupling between nanoparticle plasmons and cavity photons at ambient conditions. *Nat. Commun.* **2020**, *11*, 5561.